JOURNAL OF VIROLOGY, Aug. 2007, p. 8621–8633 Vol. 81, No. 16
0022-538X/07/$08.00+0 doi:10.1128/JVI.00759-07

Coreceptor Switch in R5-Tropic Simian/Human Immunodeficiency Virus-Infected Macaques[▽]

Siu-hong Ho,[1] Silvana Tasca,[1] Lili Shek,[1] Amy Li,[1] Agegnehu Gettie,[1] James Blanchard,[2] Daniel Boden,[1] and Cecilia Cheng-Mayer[1]*

Aaron Diamond AIDS Research Center, The Rockefeller University, 455 First Ave., 7th Floor, New York, New York 10016,[1] and Tulane National Primate Research Center, Tulane University Medical Center, 18702 Three Rivers Road, Covington, Louisiana 70433[2]

Received 9 April 2007/Accepted 17 May 2007

The basis for the switch from CCR5 to CXCR4 coreceptor usage seen in ~50% of human immunodeficiency virus type 1 (HIV-1) subtype B-infected individuals as disease advances is not well understood. Among the reasons proposed are target cell limitation and better immune recognition of the CXCR4 (X4)-tropic compared to the CCR5 (R5)-tropic virus. We document here X4 virus emergence in a rhesus macaque (RM) infected with R5-tropic simian/human immunodeficiency virus, demonstrating that coreceptor switch can happen in a nonhuman primate model of HIV/AIDS. The switch to CXCR4 usage in RM requires envelope sequence changes in the V3 loop that are similar to those found in humans, suggesting that the R5-to-X4 evolution pathways in the two hosts overlap. Interestingly, compared to the inoculating R5 virus, the emerging CXCR4-using virus is highly neutralization sensitive. This finding, coupled with the observation of X4 evolution and appearance in an animal with undetectable circulating virus-specific antibody and low cellular immune responses, lends further support to an inhibitory role of antiviral immunity in HIV-1 coreceptor switch.

The human immunodeficiency virus (HIV) enters target cells via interaction of the viral glycoprotein with the cellular receptor CD4 and two principal coreceptors, CCR5 (R5 viruses) and CXCR4 (X4 viruses) (2). Most HIV type 1 (HIV-1) transmission results in a predominantly R5 virus infection. With time, X4 variants arise and coexist with R5 virus variants in ~50% of subtype B-infected individuals, and this event is associated with rapid $CD4^+$ T-cell loss and disease progression (22, 37). The determinant(s) of phenotypic change from R5 to X4 maps largely to the V3 loop of the envelope gp120 (6, 18, 39) and can be inferred by analysis of the amino acid sequence of this region (11). Although the underlying basis for virus coreceptor switch late in infection remains ill defined, several hypotheses that include changes in target cell populations during the course of infection and/or differential immune recognition of X4 and R5 viruses have been proposed (31, 34). Furthermore, it is unclear whether X4 viruses evolve during the course of infection or are transmitted but selected against early in infection.

We have used infection of rhesus macaques (RM) with simian/human immunodeficiency viruses (SHIV) expressing the envelopes of X4 and R5 HIV-1 isolates to study the impact of coreceptor usage in virus transmission and pathogenesis. We previously reported that both X4 and R5 SHIVs can be transmitted intravenously or intravaginally but showed that the basis for the immunodeficiencies caused by these viruses is different. Whereas primary infection with X4 SHIV caused severe and sustained peripheral blood and secondary lymphoid tissue $CD4^+$ T-cell loss, infection with R5 SHIV resulted in transient loss of $CD4^+$ T cells at these sites (15, 17). Thus, infection with SHIVs of different coreceptor usage recapitulates the different stages of HIV infection in humans: R5 SHIV provides a model of early infection with gradual peripheral $CD4^+$ T cell effects, while X4 SHIV infection reproduces the precipitous $CD4^+$ T-cell decline observed in late-stage disease concomitant with the emergence of X4 virus. The R5 SHIV used in these studies, designated $SHIV_{SF162P3}$, was generated through successive rapid transfer in RM of the molecular clone $SHIV_{SF162}$, recovered from passage 3 macaque T353 after 20 weeks of infection (14). Although $SHIV_{SF162P3}$ can replicate to high titers and induce simian AIDS (SAIDS) in ~50% of infected RM by intravenous or intravaginal inoculations (reference 13 and unpublished data), no expansion or switch to CXCR4 usage has been observed with progression to disease. In the present work, we hypothesized that infection with an isolate recovered at a later stage of infection in macaque T353 may provide a greater chance of observing coreceptor switch. We reasoned this late isolate would be more diverse and divergent, allowing for rapid evolution of the viral population which may lead to a change in coreceptor preference. We tested this hypothesis by infection of RM with $SHIV_{SF162P3N}$, an R5 isolate recovered at the time of euthanasia of T353 after 66 weeks of infection.

MATERIALS AND METHODS

Cells. Human and rhesus peripheral blood mononuclear cells (PBMC) were obtained by Ficoll-Hypaque gradient purification followed by stimulation with 3 μg/ml of phytohemagglutinin A (PHA; Sigma-Aldrich, St. Louis, MO) for human PBMC (huPBMC) and 5 μg/ml staphylococcus enterotoxin B (SEB; Sigma-Aldrich) for rhesus PBMC (rhPBMC) in RPMI 1640 medium supplemented with 10% fetal bovine serum (FBS), 2 mM glutamine, 100 U/ml penicillin, 100 μg/ml streptomycin, and 20 U/ml of interleukin-2 (Novartis, Emeryville, CA). 293T cells and TZM-bl cells expressing CD4, CCR5, and CXCR4 (41) and containing integrated reporter genes for firefly luciferase and β-galactosidase under control of the HIV-1 long terminal repeat were maintained in Dulbecco's modified

* Corresponding author. Mailing address: Aaron Diamond AIDS Research Center, The Rockefeller University, 455 First Ave., 7th Floor, New York, NY 10016. Phone: (212) 448-5080. Fax: (212) 448-5158. E-mail: cmayer@adarc.org.

▽ Published ahead of print on 30 May 2007.

Eagle's medium supplemented with 10% FBS, penicillin, streptomycin, and L-glutamine. U87.CD4 cells stably expressing CD4 and one of the chemokine receptors (10) were maintained in Dulbecco's modified Eagle's medium supplemented with 10% FBS, antibiotics, 1 μg/ml puromycin (Sigma-Aldrich), and 300 μg/ml G418 (Geneticin; Invitrogen, Carlsbad, CA).

Virus isolation. $SHIV_{SF162P3N}$ was recovered by coculturing of week 66 PBMC from macaque T353 with PHA-stimulated huPBMC as previously described (26). The amplified virus was propagated in huPBMC, and the titer was determined in SEB-stimulated rhPBMC. $SHIV_{BR24N}$ was recovered by culturing of PHA-stimulated huPBMC with week 28 plasma from macaque BR24. Recovered virus as well as the control X4 $SHIV_{SF33A}$ and R5 $SHIV_{SF162P3}$ viruses were amplified and titers were determined in SEB-stimulated rhPBMCs.

Animal infection. All infections were carried out in adult RM (*Macaca mulatta*) individually housed at the Tulane National Primate Research Center in compliance with its *Guide for the Care and Use of Laboratory Animals*. Animals were confirmed to be serologically negative for simian type D retrovirus, SIV, and simian T-cell lymphotropic virus prior to infection. Intravenous inoculations were carried out with 2.4×10^3 and 4.2×10^3 50% tissue culture infectious doses of $SHIV_{SF162P3N}$ and $SHIV_{BR24N}$, respectively. Whole blood was sampled at designated time intervals. Plasma viremia was quantified by branched DNA analysis (Siemens Medical Solutions Diagnostic Clinical Lab, Emeryville, CA), and absolute $CD4^+$ and $CD8^+$ cell counts were monitored by TruCount (BD Biosciences, Palo Alto, CA). Animals with clinical signs of SAIDS were euthanized by intravenous administration of ketamine-HCl followed by an overdose of sodium pentobarbital. Tissue samples were obtained by surgery or at the time of necropsy. The percentages of $CD4^+$ T cells in the tissue samples were analyzed by flow cytometry (FACScalibur) using CD3-fluorescein isothiocyanate, CD4-phycoerythrin, and CD8-peridinin chlorophyll protein antibodies. Further phenotyping of peripheral $CD4^+$ T cells was performed by using CD28-allophycocyanin and CD95-phycoerythrin. Except for CD3-fluorescein isothiocyanate (BioSource, Camarillo, CA), all antibodies were obtained from BD Biosciences.

Determination of coreceptor usage. Blocking experiments in rhPBMC and TZM-bl cells were performed to determine coreceptor usage of replication-competent SHIVs. For rhPBMC, 1×10^6 SEB-stimulated cells were infected with 3 ng $p27^{gag}$ antigen equivalent of the indicated SHIV in the absence or presence of 1 μM of the CXCR4 inhibitor AMD3100 or CCR5 inhibitor TAK-779. After incubation for 3 h at 37°C, cells were washed and cultured in 200 μl interleukin-2 and appropriate inhibitor-supplemented RPMI medium in 96-well plates. Culture supernatants were collected over time, and $p27^{gag}$ antigen content was quantified according to the manufacturer's instructions (Coulter Corp., Miami, FL). Percentage blocking at day 7 to 10 postinfection was determined by calculating the amount of $p27^{gag}$ production in the presence relative to that in the absence of inhibitor. For TZM-bl cells, 7×10^3 cells per well of a 96-well plate were inoculated, in triplicate, with 1 ng $p27^{gag}$ antigen equivalent of the indicated SHIV in the absence or presence of inhibitors. The cells were lysed after 72 h of incubation at 37°C and processed for β-galactosidase activity according to the manufacturer's instructions (Applied Biosystems, Foster City, CA). The percentage of blocking was then determined. For assessment of coreceptor usage of reporter viruses, 7×10^3 U87.CD4.CCR5 or U87.CD4.CXCR4 cells were seeded in 96-well plates 24 h before use and infected, in triplicate, with 10 ng $p24^{gag}$ equivalent of the indicated pseudotyped viruses, followed by incubation for 72 h at 37°C. At the end of the incubation period, cells were harvested, lysed, and processed according to the manufacturer's instructions (Promega, Madison, WI). Entry, as quantified by luciferase activity, was measured with an MLX microtiter plate luminometer (Dynex Technologies, Inc., Chantilly, VA). Infection of coreceptor-bearing cells with NL4-3 virus generated in the absence of Env served as a negative control.

Neutralization assay and antibodies. Virus neutralization was assessed using TZM-bl cells in 96-well plates. Briefly, an equal volume (50 μl) of SHIV (1 ng $p27^{gag}$ equivalent) and serial dilutions of heat-inactivated macaque serum or monoclonal antibodies (MAbs) was incubated for 1 h at 37°C and then added to cells, in triplicate wells, for an additional 2 h at 37°C. A 100-μl aliquot of medium was then added to each well, and the virus-serum cultures were maintained for 72 h. Control cultures received virus in the absence of antibodies. At the end of the culture period, the cells were lysed and processed for β-galactosidase activity. A neutralization curve was generated by plotting the percentage of neutralization versus serum or MAb dilution. Results shown are representative of two independent experiments. The human MAb immunoglobulin G1b12 (IgG1b12) was obtained from D. Burton (Scripps Research Institute, La Jolla, CA), and CD4-IgG2 (PRO 542) was generously provided by Progenics Pharmaceuticals (Tarrytown, NY).

Plasmid constructs and pseudotype virus production. For expression of envelope glycoproteins, full-length gp160 coding sequences of $SHIV_{SF162P3N}$ and $SHIV_{BR24N}$ were subcloned into the pCAGGS expression plasmid to generate EnvP3N and EnvBR24N, respectively. Briefly, viral RNA was prepared from 500 μl virus supernatant using a commercially available RNA extraction kit (QIAGEN, Chatsworth, CA) and reverse transcribed with SuperScript III reverse transcriptase (Invitrogen) and random hexamer primers (Amersham Pharmacia, Piscataway, NJ). Full-length gp160 was amplified from cDNA of $SHIV_{SF162P3N}$ by primers SH43 (5′-AAGACAGAATTCATGAGAGTGAAGGGGATCAGGAAG-3′) and SH44 (5′-AGAGAGGGATCCTTATAGCAAAGCCCTTTCAAAGCCCT-3′) and from $SHIV_{BR24N}$ with primers SH52 (5′-TAGATCGAATTCTAGAGCCCTGGAAGCATCCAGGAAGTCAGCCTA-3′) and SH53 (5′-AGAGAGGGATCCTCCAGTCCCCCCTTTTCTTTTAAAAA-3′). PCR-based overlapping extension methodology was then employed to replace the V3 loop of EnvP3N with that of BR24N to generate the P3N(V3) Env expression plasmid. With EnvP3N serving as template for PCR amplification, the outer primers used were SH43 and SH44 and the inner primers were SH56 (5′-TATAATATAAGAAAAAGTATACGTATACATAGAGGACCGGGGAGAGCATTTTATGC-3′) and SH57 (5′-TCTATGTATACGTATACTTTTTCTTATATTATAGTTAGGTCTTGTACAATTAATTTCTAC-3′), which encompassed the amino acid changes found in the V3 loop of EnvBR24N (underlined) flanked by adjacent sequence. The resulting amplified fragment was verified by sequencing and subcloned back into pCAGGS. To generate luciferase reporter viruses capable of only a single round of replication, an envelope *trans*-complementation assay was used as previously described (7). P3N, BR24N, or P3N(V3) Env expression plasmid and the NL4.3LucE-R- vector were cotransfected with polyethylenimine (Polyscience, Warrington, PA) into 2.5×10^6 293T cells plated in a 100-mm plate. Cell culture supernatants were harvested 72 h later, filtered through 0.45-μm filters, and stored at −70°C in 1-ml aliquots. Pseudotype viruses were quantified for $p24^{gag}$ content (Beckman Coulter, Fullerton, CA).

DNA, RNA extraction, sequencing, and analysis. Proviral DNA was extracted from 1×10^6 to 3×10^6 PBMC with a DNA extraction kit (QIAGEN), and viral RNA was prepared from 500 μl plasma or virus supernatant as described above. The V1-to-V5 region of gp120 was amplified from the reverse transcription products by using *Taq* DNA polymerase (QIAGEN) with primers ED5 and ED12 or ES7 and ES8 as previously described (9). PCR products were cloned with the TOPO TA cloning kit (Invitrogen) per the manufacturer's instructions followed by direct automated sequencing of cloned gp120 amplicons (SeqWright, Fisher Scientific, Houston, TX). Nucleotide sequences were aligned using the CLUSTALX 1.81 program and further adjusted manually (19). Pair-wise genetic distances were calculated using Kimura's two-parameter model of molecular evolution (20). A phylogenetic tree was constructed using the maximum likelihood method, and bootstrap values were generated with 1,000 repetitions.

Sequence-specific PCR for HR insertion. Proviral and cDNA products from various time points postinfection were subjected to PCR using *Taq* DNA polymerase and primers ES7/ES8 as described elsewhere (9). Detection of HR sequence in amplified ES7/ES8 products was achieved by using primers V3-S (5′-CTGTTAAATGGCAGTCTAGC-3′) and SH30 (5′-GCTCTCCCCGGTCCTCTATG-3′) in PCRs. The cycling profile was 95°C for 15 min followed by 40 cycles of 95°C for 15 s and 72°C for 70 s. Amplified products were visualized by electrophoresis in ethidium bromide-stained 2% agarose gels. Appropriate mixing and titration experiments with R5 and X4 variant target sequences that differ in the HR region were performed. The sensitivity of the detection assay was shown to be one X4 variant copy in 10^6 R5 targets.

RESULTS

High levels of virus replication in macaques infected with the late isolate $SHIV_{SF162P3N}$. We hypothesized that a late-stage SAIDS-associated CCR5-tropic SHIV isolate, being more diverse and divergent, replicates better and evolves more rapidly than an earlier isolate, providing a greater chance of observing coreceptor switch. To test this hypothesis, we first determined the genetic composition of $SHIV_{SF162P3N}$, an R5 isolate recovered after the onset of SAIDS (week 66), and compared it to the parental clone, $SHIV_{SF162}$, as well as the earlier isolate, $SHIV_{SF162P3}$. Sequence analysis revealed that $SHIV_{SF162P3N}$ is indeed more divergent from the parental clone than is the week 20 $SHIV_{SF162P3}$ virus (Fig. 1A) and is more diverse (Fig. 1B). The average genetic distances among

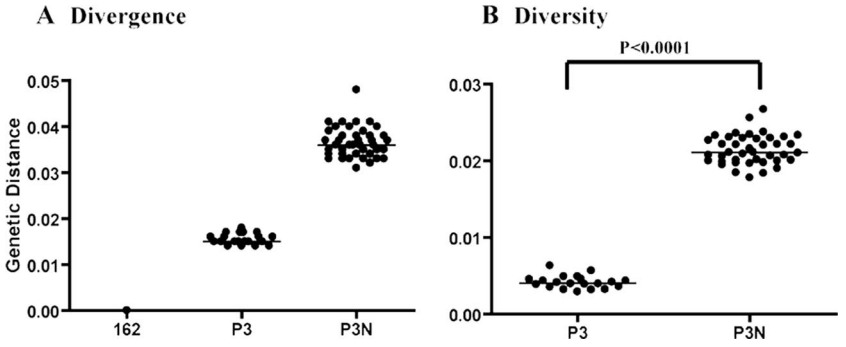

FIG. 1. Divergence and diversity of the late week 66 isolate $SHIV_{SF162P3N}$. (A) Viral divergence from the founder clone $SHIV_{SF162}$ (162) of $SHIV_{SF162P3}$ (P3) and $SHIV_{SF162P3N}$ (P3N). The V1-V5 Env gp120 sequence for 20 and 41 clones of P3 and P3N, respectively, was determined. Nucleotide sequences were aligned and the means and standard deviations for all pair-wise comparisons between the sequences of the two isolates and the molecular clone 162 were then calculated using Kimura's two-parameter model of molecular evolution (20). (B) Viral population diversity of P3 and P3N. Genetic distances between all possible pairs of Env nucleotide sequences for viral RNA in the two virus inocula are shown. Bars indicate median values. The *P* value is from an unpaired *t* test.

the Env clones sequenced are greater for the week 66 isolate than the week 20 isolate ($P < 0.0001$). Three RM were then inoculated intravenously with $SHIV_{SF162P3N}$. Infection was established in all three macaques, with peak plasma viremia of 10^6 to 10^7 RNA copies/ml by 2 weeks postinfection (wpi) (Fig. 2A). Viral replication declined thereafter in two macaques (CD80 and T799) but rebounded by 10 wpi, reaching set points of 10^5 to 10^6 RNA copies/ml plasma. A transient drop in peripheral $CD4^+$ T cells, characteristic of R5 SHIV infection (17), accompanied peak infection but recovered close to preinfection values by 8 wpi. With the rise in viremia at 10 wpi, progressive $CD4^+$ T-cell decline followed, which was less protracted in CD80 than T799. Both macaques seroconverted by 6 wpi (Table 1), and peripheral SIV Gag-specific gamma interferon-secreting $CD8^+$ T cells could be detected by intracellular cytokine staining (data not shown). CD80 developed clinical signs consistent with SAIDS and was euthanized at 66 wpi. At the time of death, CD80 had viral loads of $>10^5$ RNA cop-

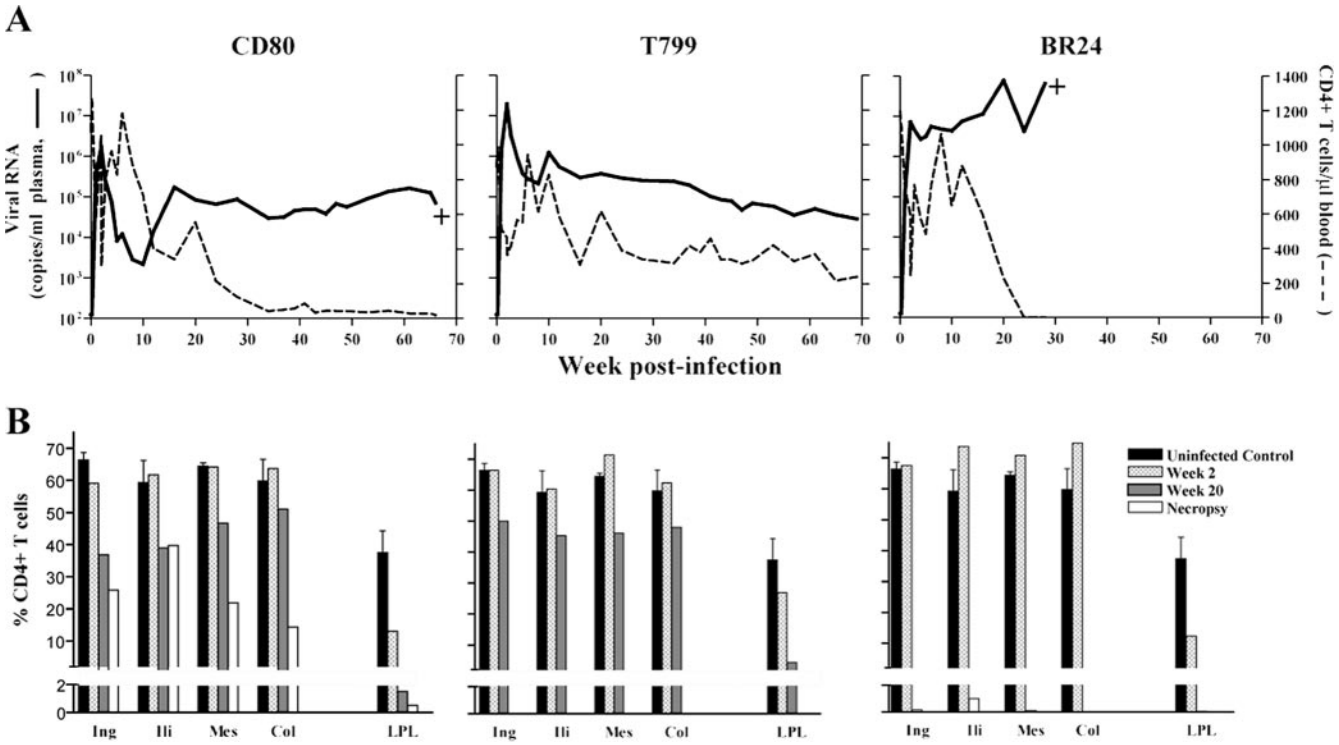

FIG. 2. Virologic and immunologic measurements in R5 $SHIV_{SF162P3N}$-infected RM CD80, T799, and BR24. (A) Viral load and absolute $CD4^+$ T-cell counts. (B) Percentages of $CD4^+$ T cells in the inguinal (Ing), iliac (Ili), mesenteric (Mes), and colonic (Col) lymph nodes and LPLs from the jejunum during peak (week 2) and chronic (week 20) stages of infection and at time of necropsy. Baseline values generated from three uninfected macaques are shown for reference. +, death due to euthanasia. Surgery was not performed on BR24 at week 20 due to the development of clinical signs consistent with SAIDS.

TABLE 1. Humoral immune response in $SHIV_{SF162P3N}$-infected macaques

RM	Protein	Antibody response at wpi[a]:			
		0	6	12	28
BR24	gp120	−	−	−	−
	gp41	−	−	−	−
	p31	−	−	−	−
	p27	−	−	−	−
CD80	gp120	−	++++	++++	++++
	gp41	−	++++	++++	+++
	p31	−	−	++	++
	p27	−	++++	++++	+++
T799	gp120	−	++++	++++	++++
	gp41	−	++++	++++	+++
	p31	−	+	+++	++
	p27	−	++++	++++	++

[a] SHIV-specific antibody responses were detected using the strip immunoblot assay in accordance with the manufacturer's instructions (Novartis, Emeryville, CA). Macaque sera reactivity was determined by comparison with two internal IgG strip controls. Scoring relative to level I and II control bands was as follows: −, an absent band; ±, intensity lower than the level I band; +, intensity equal to the level I band; ++, intensity greater than the level I but less than the level II band; +++, intensity equal to the level II band; ++++, intensity greater than the level II band.

ies/ml of plasma and a $CD4^+$ T-cell count of 19 cells/μl of blood. Histopathological findings included multifocal, lymphoid hyperplasia of peripheral and iliac lymph nodes, thymic atrophy, and multiple opportunistic infections (*Cryptosporidium*, *Helicobacter pylori*, and *Microsporidia*).

The third infected RM, BR24, demonstrated a rapid progressor phenotype. This macaque had sustained viremia that was 2 logs higher ($\sim 10^7$ RNA copies/ml plasma) and failed to develop strong antiviral immune responses. Circulating virus-specific antibody was undetectable (Table 1), and the response of peripheral $CD8^+$ T cells to stimulation with SIV Gag peptides was low and intermittent (data not shown). After a period of transient acute loss, peripheral $CD4^+$ T-cell counts in BR24 also recovered to within the normal range up to 16 wpi but dropped precipitously thereafter. Concomitant with the onset of rapid $CD4^+$ T-cell loss was a spike in viremia to $>10^8$ RNA copies/ml of plasma at 20 wpi. BR24 was euthanized at week 28 with clinical signs of SAIDS. At necropsy, BR24 showed histopathological lesions that included severe lymphoid depletion of peripheral and alimentary lymph nodes along with generalized inflammation, thymic dysinvolution, and opportunistic infections (*Crytosporidium* and *Pneumocystis carinii*). The circulating $CD4^+$ T-cell count in this animal at the time of death was 1 cell/μl of blood.

Analyses of the percentages of $CD4^+$ T cells in tissue compartments during peak (2 wpi) and chronic (20 wpi) infection in CD80 and T799 revealed moderate $CD4^+$ T-cell loss (<30%) in peripheral lymph nodes (LN) but close to a 90% drop in $CD4^+$ T lymphocytes at effector sites such as the lamina propria (LP) of the gut by 20 wpi (Fig. 2B). At necropsy, >99% of $CD4^+$ T lymphocytes in the gut of CD80 were depleted, but with preservation of 15 to 40% $CD4^+$ T cells in all secondary lymphoid tissues examined. A similar pattern of peak $CD4^+$ T cells loss was observed in macaque BR24, with depletion only in the gut at 2 wpi (Fig. 2B). At necropsy, however, there was massive depletion of LN $CD4^+$ T cells as well as LP lymphocytes (LPL). This pattern of severe $CD4^+$ T-cell loss differs from CD80 and is reminiscent of that seen in X4 SHIV-infected macaques (17), raising the possibility of X4 emergence in BR24. To investigate this possibility, virus was recovered from BR24 plasma obtained at necropsy. The coreceptor usage of the recovered virus, designated $SHIV_{BR24N}$, was then determined.

Emergence of a CXCR4-using and neutralization-sensitive variant in macaque BR24. We confirmed CCR5 usage of $SHIV_{SF162P3}$ and $SHIV_{SF162P3N}$ by demonstrating that the CCR5 inhibitor TAK-779 and not the CXCR4 inhibitor AMD3100 blocked replication of these viruses in rhPBMC (Fig. 3A). In contrast, replication of $SHIV_{BR24N}$, similar to the X4 $SHIV_{SF33A}$ virus, was not inhibited by TAK-779 but was completely blocked by AMD3100. Similar results were obtained using TZM-bl cells (Fig. 3B), showing that $SHIV_{BR24N}$ uses CXCR4 for entry in vitro. Because a recent report indicated that increased neutralization sensitivity of CXCR4-using HIV-1 strains emerged during the transition from CCR5 to CXCR4 usage (4), the susceptibility of $SHIV_{BR24N}$ to antibody neutralization was also examined. Compared to the inoculating R5 $SHIV_{SF162P3N}$ virus, we found that the X4 $SHIV_{BR24N}$ isolate is highly sensitive to neutralization with sera from ma-

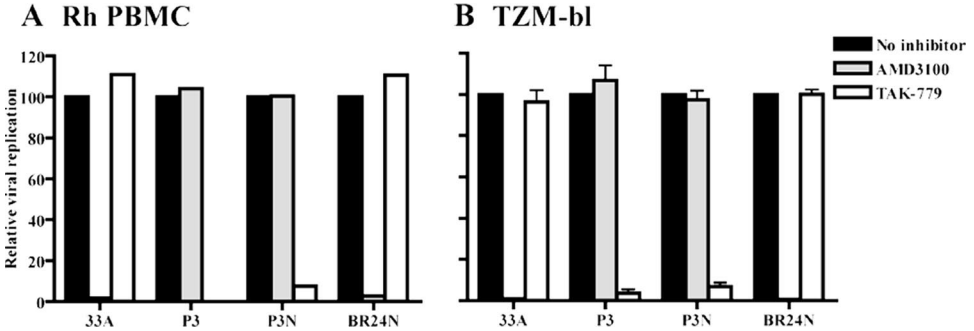

FIG. 3. Coreceptor usage of $SHIV_{BR24N}$. CXCR4 and CCR5 usage of the inoculating virus $SHIV_{SF162P3N}$ (P3N) and $SHIV_{BR24N}$ (BR24N), the virus recovered from BR24 at end-stage disease, was determined by blocking entry into rhPBMC (A) and TZM-bl (B) cells with 1 μM CXCR4-specific (AMD3100) or CCR5-specific (TAK-779) inhibitor. X4 $SHIV_{SF33A}$ (33A) and R5 $SHIV_{SF162P3}$ (P3) served as controls. For TZM-bl cells, error bars indicate standard errors of data in triplicate wells. Results shown are representative of at least two independent experiments, and for rhPBMC cells from two different animals were used.

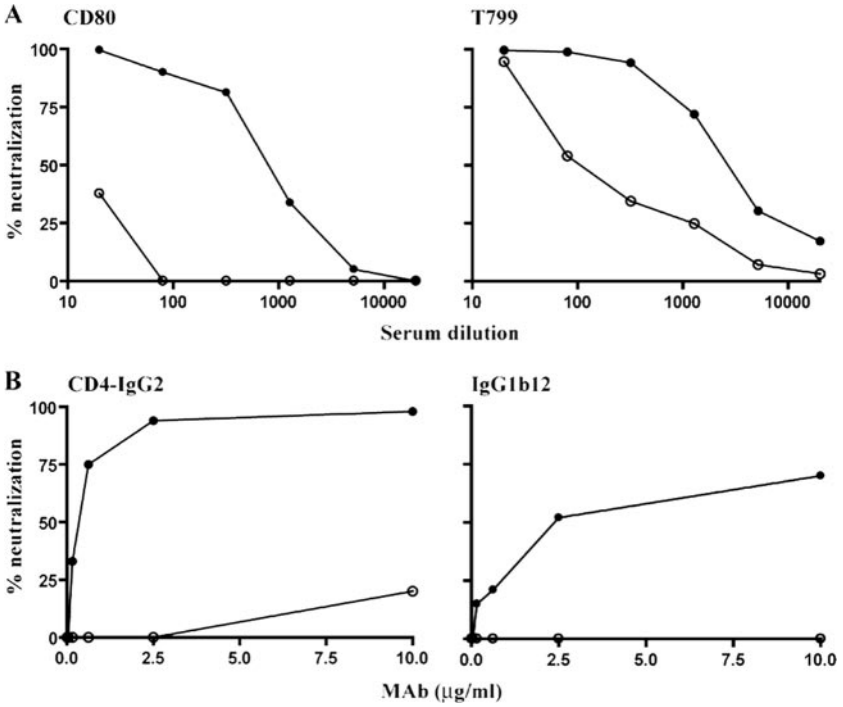

FIG. 4. Neutralization sensitivity of $SHIV_{SF162P3N}$ and $SHIV_{BR24}$. The neutralization susceptibilities of the inoculating R5 $SHIV_{SF162P3N}$ (○) and emerging X4 $SHIV_{BR24}$ (●) viruses to antibodies in sera from macaques CD80 and T799 (A) and CD4 binding site MAbs CD4-IgG2 and IgG1b12 (B) were determined as described in Materials and Methods. Data shown are representative of at least two independent neutralization experiments.

caques CD80 and T799 (Fig. 4A). A 90% neutralization of $SHIV_{BR24N}$ was achieved at dilutions of 1:160 and 1:1,280 of CD80 and T799 sera, respectively. In contrast, the R5 $SHIV_{SF162P3N}$ inoculating virus was resistant to neutralization with serum from macaque CD80, while a similar degree of neutralization (90%) with T799 serum required a 32-fold-higher titer (1:40). $SHIV_{BR24N}$ is also more sensitive than $SHIV_{SF162P3N}$ to neutralization with the broadly cross-reactive CD4 binding site monoclonal antibodies CD4-IgG2 and IgG1b12 (Fig. 4B). CD4-IgG2 potently neutralized $SHIV_{BR24N}$ at concentrations of 2 μg/ml, while IgG1b12 achieved 70% neutralization at the highest concentration tested (10 μg/ml). These CD4 binding site MAbs, however, were unable to neutralize $SHIV_{SF162P3N}$. Collectively, the data showed emergence of a neutralization-sensitive CXCR4-utilizing variant in macaque BR24.

Sequence of the $SHIV_{BR24N}$ variant envelope gp120. We sequenced and compared the envelope gp120 V1-to-V5 region of the inoculating R5 $SHIV_{SF162P3N}$ virus and the X4 $SHIV_{BR24N}$ variant to understand their relationship (Fig. 5A). All $SHIV_{BR24N}$ Env clones sequenced (22 in total) harbored the same nine unique amino acid changes compared to the inoculating strain. Two of the changes are in the V2 region and two are in the C4 region, with five clustering in the V3 domain. The nonsynonymous serine-to-arginine change in V2 as well as the asparagine-to-tyrosine and threonine-to-isoleucine changes in V3 are predicted to result in loss of potential N-linked glycosylation sites in these regions of the $SHIV_{BR24N}$ envelope gp120. Furthermore, insertion of two positively charged amino acids, histidine and arginine immediately upstream of the GPGR crown V3 loop sequence, increases the overall charge of this domain, and the two amino acid changes in C4 are within a conserved gp120 structure implicated in CCR5 binding (35). The conservation of this particular set of changes in regions known to influence envelope functions, including coreceptor usage (23, 36), points to their importance in determining the phenotypic characteristics of the $SHIV_{BR24N}$ variant. Phylogenetic tree analysis of Env V1-V5 sequences showed two loosely clustered viral populations within the inoculating $SHIV_{SF162P3}$ virus (Fig. 5B). The $SHIV_{BR24N}$ sequences, although limited in diversity, are markedly divergent from those of the inoculum, with the branching point of variant-associated sequences having its origin within one of the inoculating R5-associated subpopulations (100% bootstrap value). Collectively, the data support derivation of the X4 $SHIV_{BR24N}$ variant from the inoculating R5 virus.

The V3 loop of $SHIV_{BR24N}$ dictates CXCR4 usage. The V3 domain of HIV-1 gp120 is known to contribute to coreceptor use. A closer examination of this region revealed the presence of two major V3 loop species each representing 14 of 41 Env clones sequenced in the R5 $SHIV_{SF162P3N}$ virus inoculum (Fig. 6A) but homogeneity in the recovered X4 $SHIV_{BR24N}$ virus. As predicted, the overall positive charge of this region of gp120 is higher for $SHIV_{BR24N}$ (+9) than $SHIV_{SF162P3N}$ (+6 or +7), but basic amino acids at V3 positions 11 and 25 that frequently distinguish primary X4 and R5 viruses (11) were absent in $SHIV_{BR24N}$. Of note, insertion of the two basic amino acids (histidine and arginine) at the crown of the loop was at the same position as those found in the prototypic X4 HIV-1 strains HXB2 and Ams-32. Furthermore, the N-terminal glycan, which has been shown to modulate antibody neutraliza-

tion susceptibility and interaction of HIV-1 Env with chemokine receptors (1, 27, 33), is lost in both $SHIV_{BR24N}$ and Ams-32. The lack of the N-terminal V3 loop glycan in $SHIV_{BR24N}$ envelope gp120 likely contributes to increased sensitivity of the virus to serum as well as CD4-IgG2 and IgG1b12 neutralization.

To determine whether the V3 loop of $SHIV_{BR24N}$ determines CXCR4 usage, the 37-amino-acid V3 domain of this virus was used to replace the corresponding region of $SHIV_{SF162P3N}$ gp120 (EnvP3N) to generate the recombinant EnvP3N(V3). In single-round infectivity assays, we found that, contrary to EnvP3N, the recombinant EnvP3N(V3) was not able to mediate entry into U87.T4 cells expressing CCR5 (Fig. 6B). Instead, similar to the envelope of $SHIV_{BR24N}$ (EnvBR24N), EnvP3N(V3) used CXCR4 as the coreceptor. Taken together, the data demonstrate that the V3 loop of $SHIV_{BR24N}$ is a major determinant of coreceptor preference.

Tracking X4 evolution and emergence in macaque BR24. The presence of the two amino acid insertions in the V3 loop of $SHIV_{BR24N}$ allows for the design of PCR primers that can distinguish between the inoculating R5 virus and the X4 variant to track evolution of the latter in macaque BR24. Signature X4 variant "HR" sequence could not be detected in the $SHIV_{SF162P3N}$ inoculum (data not shown) or at early times in the infection of macaque BR24 (Fig. 7). It was first detected in both plasma and PBMC of BR24 at 20 wpi, coinciding with the spike in viremia. Interestingly, although X4 emergence was associated with loss of peripheral $CD4^+$ T cells and disease progression, it appeared to occur after the onset of precipitous peripheral $CD4^+$ T-cell decline seen at weeks 12 to 16.

$SHIV_{BR24N}$ uses CXCR4 in vivo. To establish coreceptor usage of $SHIV_{BR24N}$ in vivo, two macaques were inoculated intravenously with cell-free virus. Both animals were infected, and peak viremia in CP93 (10^6 RNA copies/ml plasma) was 1 log lower than in CT43 (Fig. 8A). A rapid and sustained drop in peripheral $CD4^+$ T cells that was more dramatic for CT43 than CP93 and accompanied virus replication. Examination of the percentages of tissue $CD4^+$ T cells during peak infection (3 wpi) showed >70% loss in all LN of CP93 examined but little or no loss in the gut (Fig. 8B). In CT43, the macaque with a 1-log-higher peak viremia, massive depletion (>98%) of $CD4^+$ T cells was seen in the LN, with substantial depletion in the gut as well. Although the extent of $CD4^+$ T-cell loss among the two $SHIV_{BR24N}$-infected macaques varied due to a difference in viral load, the pattern and sites of $CD4^+$ T-cell depletion are similar to those found in X4-infected and not R5 SHIV-infected macaques (Fig. 2B) (17). Analyses of the circulating T-cell subpopulations showed early targeting and depletion of naïve $CD4^+$ T cells, where the rate of loss of this T-cell subset paralleled the $CD4^+$ T-cell drop (Fig. 8C). Naïve $CD4^+$ T lymphocytes express high levels of CXCR4 but not CCR5 (3, 17). Thus, the in vivo findings corroborated the in vitro data, showing CXCR4 usage of $SHIV_{BR24N}$.

DISCUSSION

This report documents phenotypic coreceptor switch in an animal model of HIV/AIDS. Functional, sequence, and in vivo

FIG. 5. (A) Env V1-V5 amino acid sequence comparison of $SHIV_{SF162P3N}$ and $SHIV_{BR24N}$. Sequences of 41 $SHIV_{SF612P3N}$ and 22 $SHIV_{BR24N}$ Env clones were aligned with the reference $SHIV_{SF162}$ (GenBank accession number M38428) and the consensus $SHIV_{SF162P3}$ (GenBank accession number AF536757) sequences. Gaps are indicated by wave lines and dots denote identical residues in the sequence. Potential N-linked glycosylation sites are bracketed, and the nine unique amino acid changes shared by all the BR24N sequences are shaded in yellow. The numbers shown on the right of a sequence represent the number of clones containing this sequence out of the total number of clones sequenced. Those lacking numbers on the right represent unique sequences. (B) Phylogenetic tree showing the relationship between the $SHIV_{162P3N}$ and $SHIV_{BR24N}$ sequences. A maximum likelihood tree rooted on the sequence of the molecular clone $SHIV_{SF162}$ was generated. The scale bar indicates the genetic distance along the horizontal branches, and the numbers at the nodes are bootstrap values.

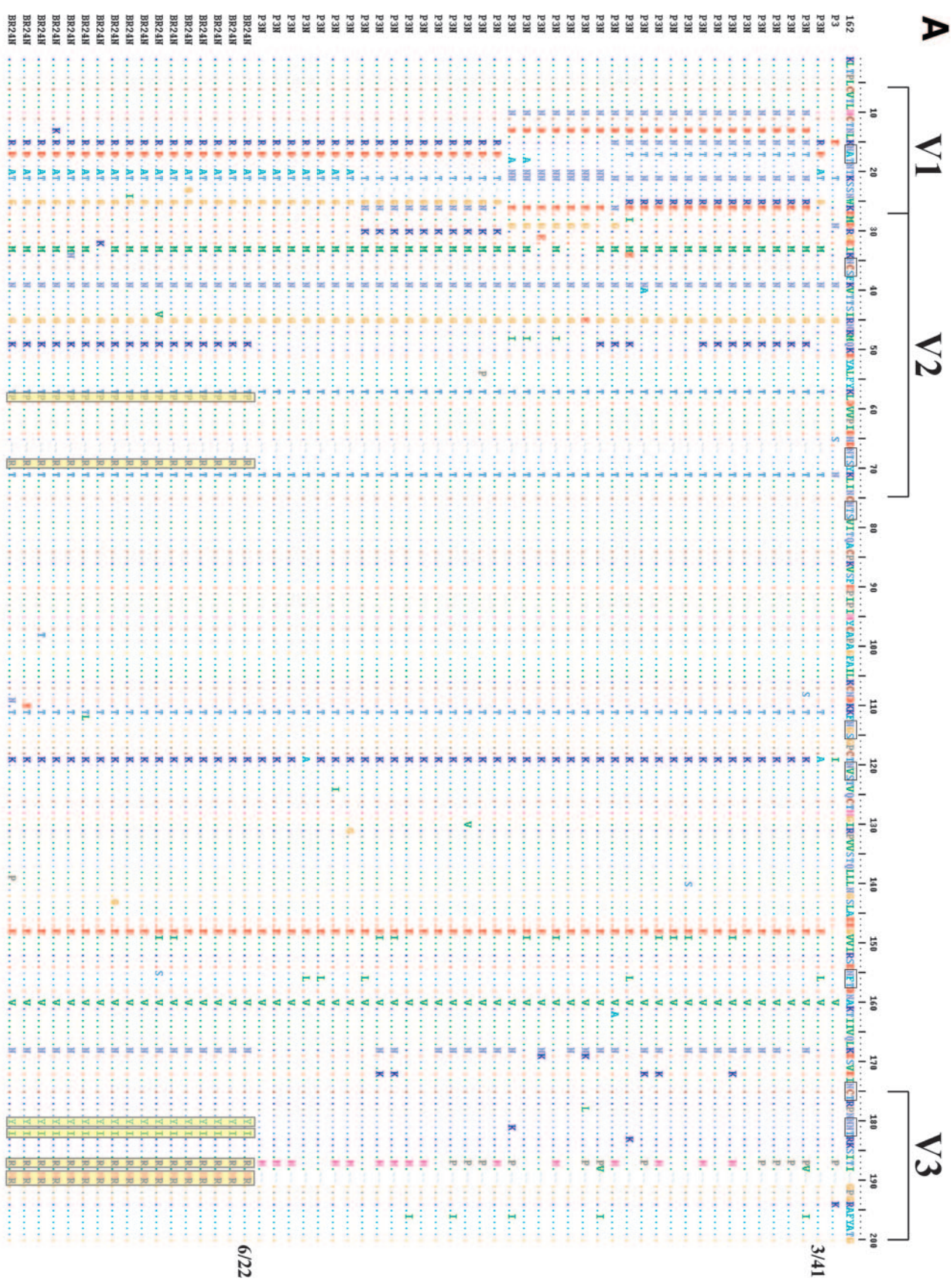
A
V1
V2
V3
3/41
6/22

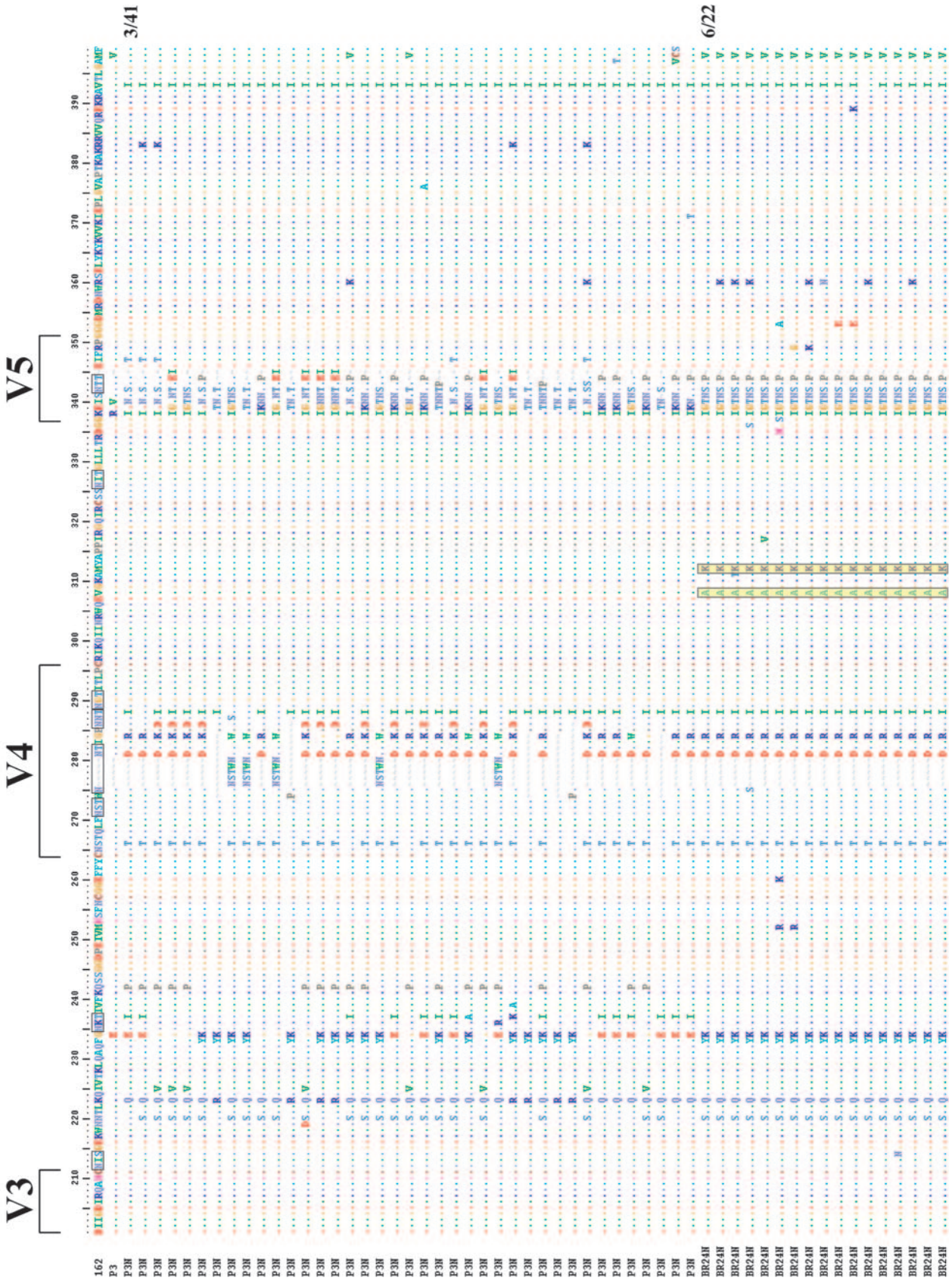
V3
V4
V5
3/41
6/22

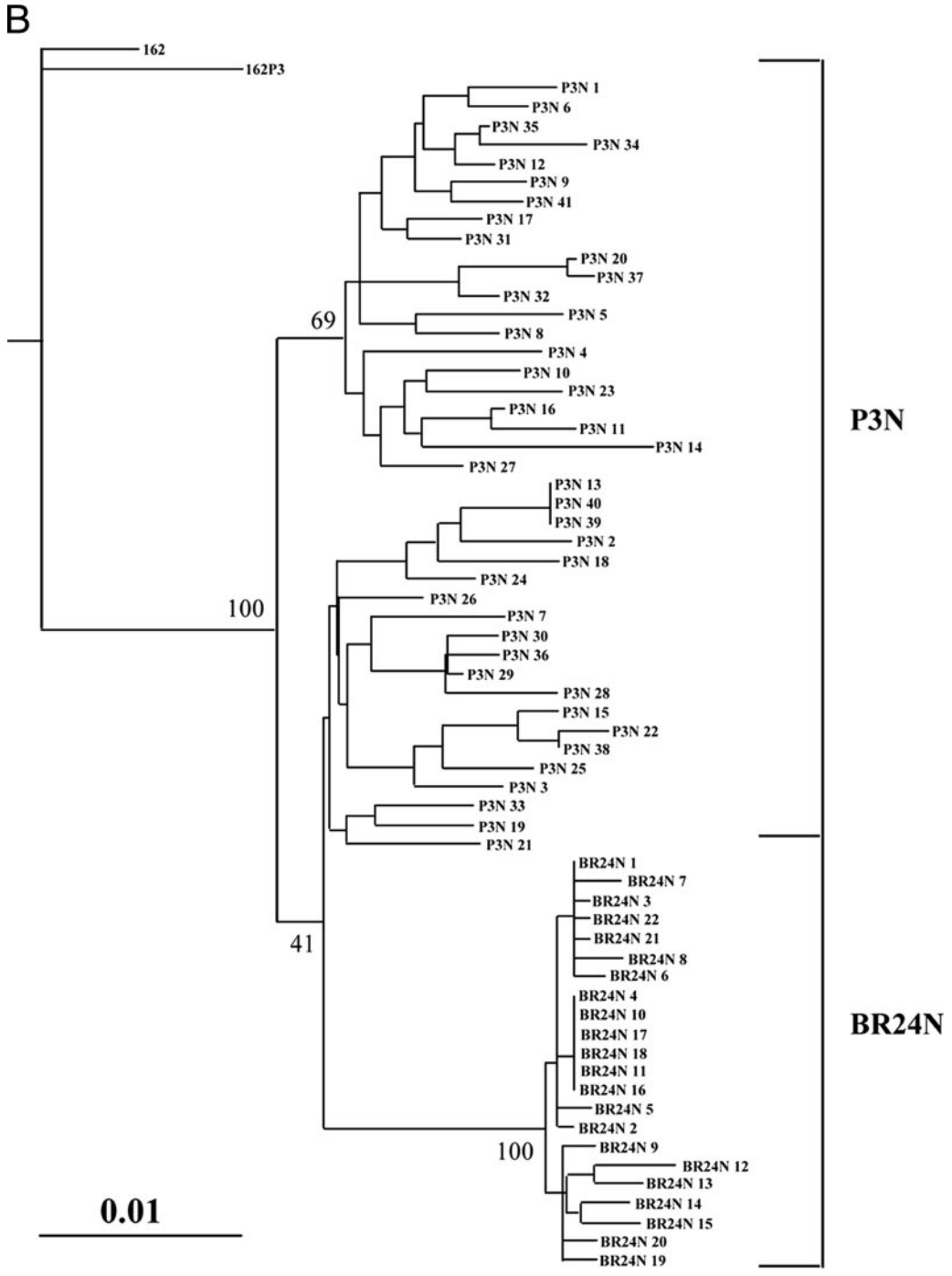

FIG. 5—*Continued*.

infectivity studies showed that contrary to the inoculating strain, R5 $SHIV_{SF162P3N}$, the virus recovered at end-stage disease of macaque BR24 uses CXCR4 for entry. Although it is formally possible that the X4 variant is present in the inoculum at an extremely low level, the temporal correlation between the appearance of the X4 variant, the spike in viremia, and progression to disease, coupled with the phylogenetic relationship between the variant and the inoculating R5 $SHIV_{SF162P3N}$ virus as well as the inability to detect the X4 variant signature sequence in the inoculum with sequence-specific PCR that has a sensitivity of detection of 1 in 10^6 copies, strongly suggests that evolution to CXCR4 usage occurred in macaque BR24.

The mechanism(s) for X4 emergence late in infection has been debated for many years. Various frequencies of X4 viruses have been reported throughout the course of HIV-1 natural infection (38), but their dominance is seen only towards the end stage of disease. We and others previously proposed an immunological restriction on coreceptor switch

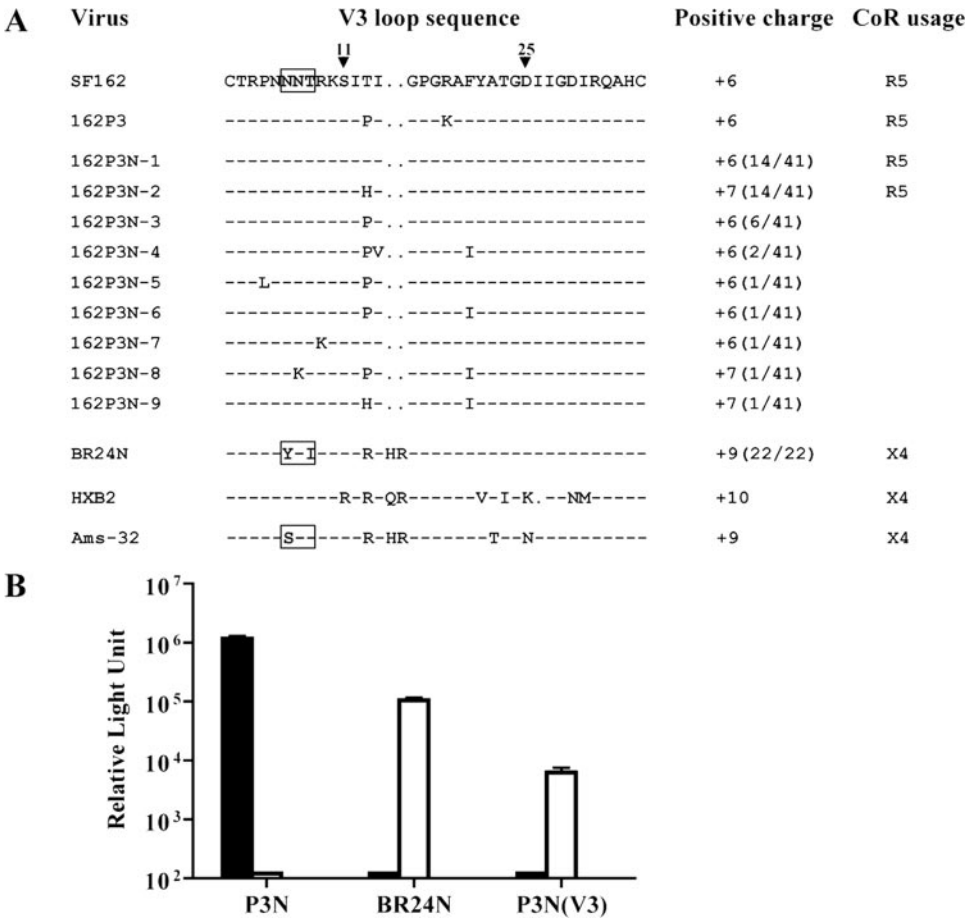

FIG. 6. (A) Comparison of V3 loop sequences of $SHIV_{162P3N}$, $SHIV_{BR24N}$, and well-characterized X4 and R5 viruses. Gaps are indicated as dots, dashes denote similarities in sequence, and the total positive charge of this region was calculated and is shown. Positions 11 and 25 within the V3 loop are indicated, and the N-terminal glycan site is bracketed. The numbers in parentheses represent the number of clones with the indicated V3 loop sequence per the total number sequenced. (B) Relative entry into U87.T4.CCR5 cells (black bars) and U87.T4.CXCR4 cells (white bars) of luciferase reporter viruses expressing the envelope of $SHIV_{SF162P3N}$ (EnvP3N), $SHIV_{BR24N}$ (EnvBR24N), and V3 loop recombinant EnvP3N(V3). All data are the means of triplicates + standard errors of the means.

that is based on the assumption that the X4 virus is more susceptible to immune control (13, 29). The appearance of X4 variants late in infection, therefore, is presumed to be the consequence rather than the cause of the collapse of the host immune system. In this regard, our findings of evolution and emergence of neutralization-sensitive X4 variants in an R5 SHIV-infected macaque with undetectable antiviral antibody responses are of interest. Increased neutralization sensitivity of

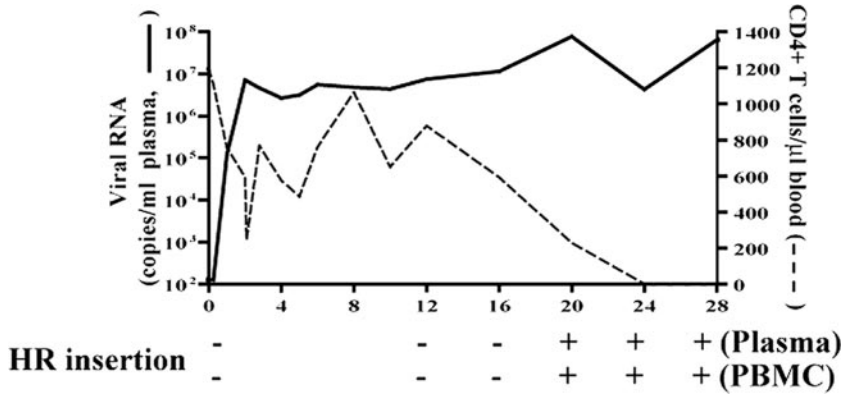

FIG. 7. Evolution of X4 variants in macaque BR24 as tracked by the presence of the signature V3 HR insertion sequence, using sequence-specific PCR. + and − indicate presence and absence of the insertion.

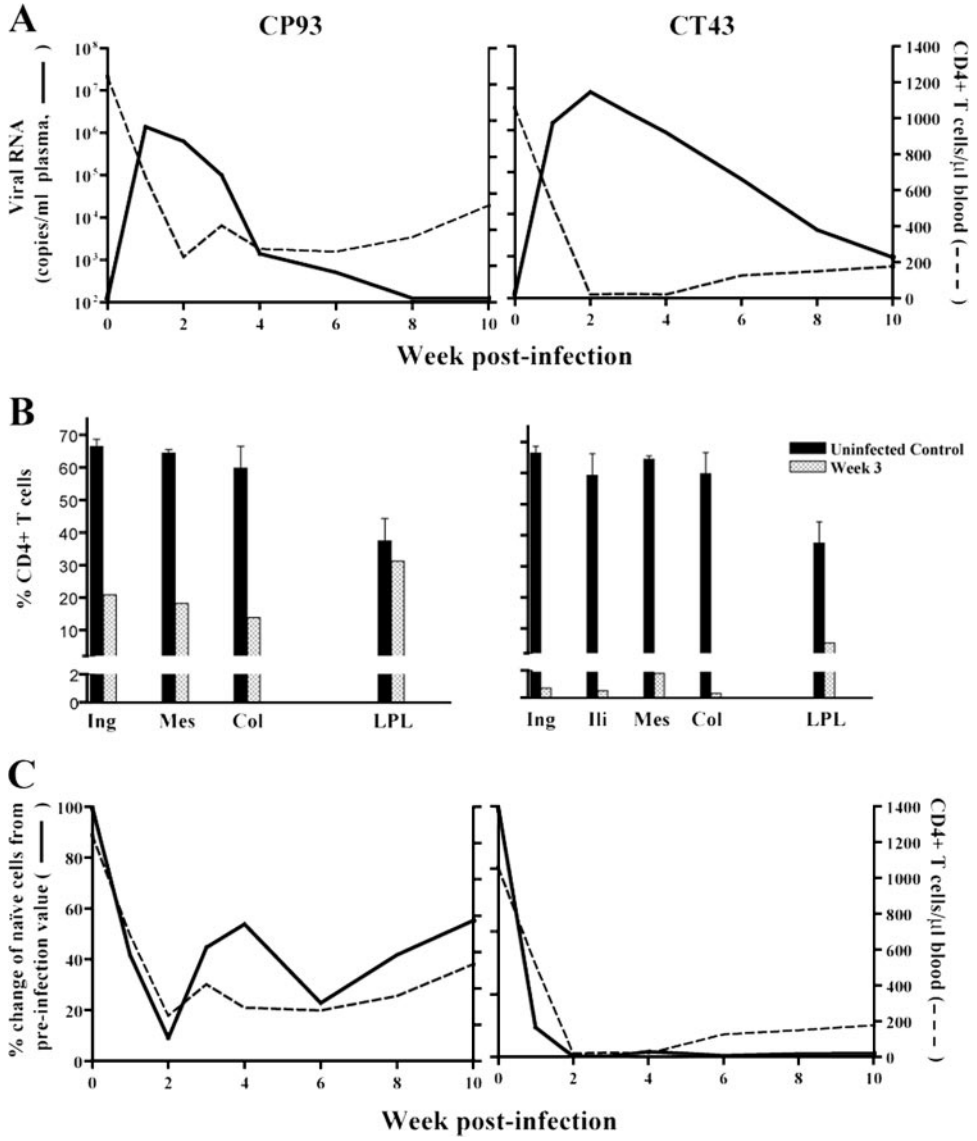

FIG. 8. Virologic and immunologic measurements in $SHIV_{BR24N}$-infected RM. (A) Viral load and absolute $CD4^+$ T-cell counts. (B) Percentage of $CD4^+$ T cells in various lymphoid compartments and the gut LPL after 3 weeks of infection. Baseline values generated from three uninfected macaques are shown for reference. (C) Percent change of naïve $CD4^+$ T cells as identified by the $CD95^{low}$ $CD28^{high}$ phenotype in peripheral blood of BR24. The baseline naïve $CD4^+$ T-cell subset value for each macaque was set at 100%.

recently emerged CXCR4-using HIV-1 variants has also been reported (4). This, together with data indicating similar V3 sequence changes associated with CXCR4 usage in $SHIV_{BR24N}$ and the HIV-1 isolate Ams-32, raises the possibility that similar mechanistic pathways underlie phenotypic conversion in some HIV-1-infected patients and macaques. We suggest that adaptation to efficient usage of CXCR4 requires conformational changes in the envelope glycoprotein, such as the loss of the N-terminal V3 loop glycan (1, 27, 33), that may render the virus more susceptible to antibody neutralization. In the absence of such immune selection pressures in the rapid progressor BR24, or in patients with end-stage disease, the X4 variants that evolved during the course of infection can now emerge and subsequently dominate. Further studies on the impact of amino acid changes in the V2, V3, and C4 regions of $SHIV_{BR24N}$ envelope gp120 on virus entry, receptor usage efficiency, and neutralization susceptibility should further our understanding of the basis for the late appearance of X4 viruses.

Surprisingly, emergence of the X4 variant in macaque BR24 appears to follow rather than precede or coincide with the onset of precipitous peripheral $CD4^+$ T-cell loss. Similar observations have also been made in HIV-1-infected infants and adults (5, 32). It is conceivable that X4 viruses are present at the time of accelerated $CD4^+$ T-cell decline in macaque BR24 but are below the limit of detection or in anatomical sites, such as the lymph nodes and thymus, that were not sampled. This scenario supports the idea that X4 emergence is the cause of the rapid loss of total $CD4^+$ T cells. Alternatively, even though circulating virus-specific antibody and the cytokine-producing

$CD8^+$ T-cell response is either absent or at low levels, the presence of antiviral immunity at lymphoid and/or mucosal tissue compartments early in infection cannot be excluded. Thus, it is tempting to speculate that the onset of the rapid drop in peripheral $CD4^+$ T cells seen in macaque BR24 at 16 wpi is due to further impairment of the suppressive capacity of the immune system as a consequence of sustained high-level viral replication. The final collapse of the immune system removes any selection pressures acting against X4 viruses, allowing for their emergence at 20 wpi. This latter interpretation of the observation is consistent with the notion that X4 appearance is the result, rather than the cause of, immune failure. Although we cannot formally exclude a contribution of target cell availability to the phenotypic switch in BR24, we deem this possibility less likely given that CCR5-expressing cells were also limiting in macaque CD80 at end-stage disease, but X4 virus failed to emerge in this seropositive animal. Target cell availability has also been suggested not to be a driving force for the R5-to-X4 switch in HIV-1-infected individuals (40).

In vitro, two amino acid residue changes in the V3 domain of HIV-1 strain SF162 are sufficient to expand to CXCR4 usage (8, 16, 21). The same two V3 mutations are seen for multiple CXCR4-using variants selected either by target cell limitation or CCR5 inhibition, leading to the conclusion that SF162 has a single pathway for acquiring CXCR4 use (21). We show here that coreceptor switch of a SHIV molecular clone expressing the SF162 envelope in RM requires amino acid residue changes in the V3 loop that are different from those reported in tissue culture systems. The need to escape evolving immune selective pressures while at the same time maintaining viral fitness and efficient coreceptor usage on diverse tissue cells of the macaque host likely explains the differences in sequence change required for adaptation of the SF162 envelope to function with CXCR4 in vivo and in vitro. Whether intermediates between CCR5 and CXCR4 use are involved in the R5-to-X4 evolutionary process in vivo, as well as the costs and benefits in expanding or switching coreceptor usage on virus receptor binding and replication fitness, merits further investigation.

The identification of an R5 SHIV that can switch to CXCR4 usage in infected RM through genetic adaptations similar to those seen in humans holds promise in providing the experimental tool critically needed to fully elucidate the mechanistic basis for and obstacles to coreceptor switch in HIV-1 infection. The coreceptor switch we observed was in an animal with rapid disease progression, a clinical course that is rarely seen in HIV-1-infected individuals (12, 25, 28, 30). Accordingly, it will be important to demonstrate that coreceptor switch occurs in additional $SHIV_{SF162P3N}$-infected macaques, especially in conventional progressors. Nevertheless, the experimental system can be employed to examine whether administration of antibodies to CD8 T cells or B cells that perturb the immune system to artificially promote a rapid progressor condition, or CCR5 blockers (24) to alter target cell availability at or during the course of $SHIV_{SF162P3N}$ infection of RM, hastens the process of X4 virus evolution and emergence, which inevitably heralds an unfavorable clinical outcome.

ACKNOWLEDGMENTS

We thank Lisa Chakrabarti and Jay Levy for discussions and critical comments, Zhiwei Chen for help with phylogenetic tree analysis, and Lily Tsai for help with the strip immunoblot analysis. AMD3100, TAK779, and TZM-bl cells and the U87.CD4 indicator cell line were obtained through the NIH AIDS Research and Reference Reagent Program.

This work was supported by National Institutes of Health grants R01AI46980 and R37AI41945.

REFERENCES

1. **Back, N. K., L. Smit, J. J. De Jong, W. Keulen, M. Schutten, J. Goudsmit, and M. Tersmette.** 1994. An N-glycan within the human immunodeficiency virus type 1 gp120 V3 loop affects virus neutralization. Virology **199:**431–438.
2. **Berger, E. A.** 1997. HIV entry and tropism: the chemokine receptor connection. AIDS **11**(Suppl. A)**:**S3–S16.
3. **Bleul, C. C., L. Wu, J. A. Hoxie, T. A. Springer, and C. R. Mackay.** 1997. The HIV coreceptors CXCR4 and CCR5 are differentially expressed and regulated on human T lymphocytes. Proc. Natl. Acad. Sci. USA **94:**1925–1930.
4. **Bunnik, E. M., E. D. Quakkelaar, A. C. van Nuenen, B. Boeser-Nunnink, and H. Schuitemaker.** 2007. Increased neutralization sensitivity of recently emerged CXCR4-using human immunodeficiency virus type 1 strains compared to coexisting CCR5-using variants from the same patient. J. Virol. **81:**525–531.
5. **Casper, C., L. Naver, P. Clevestig, E. Belfrage, T. Leitner, J. Albert, S. Lindgren, C. Ottenblad, A. B. Bohlin, E. M. Fenyo, and A. Ehrnst.** 2002. Coreceptor change appears after immune deficiency is established in children infected with different HIV-1 subtypes. AIDS Res. Hum Retrovir. **18:**343–352.
6. **Cocchi, F., A. L. DeVico, A. Garzino-Demo, A. Cara, R. C. Gallo, and P. Lusso.** 1996. The V3 domain of the HIV-1 gp120 envelope glycoprotein is critical for chemokine-mediated blockade of infection. Nat. Med. **2:**1244–1247.
7. **Connor, R. I., B. K. Chen, S. Choe, and N. R. Landau.** 1995. Vpr is required for efficient replication of human immunodeficiency virus type-1 in mononuclear phagocytes. Virology **206:**935–944.
8. **Dejucq, N., G. Simmons, and P. R. Clapham.** 2000. T-cell line adaptation of human immunodeficiency virus type 1 strain SF162: effects on envelope, vpu and macrophage-tropism. J. Gen. Virol. **81:**2899–2904.
9. **Delwart, E. L., and C. J. Gordon.** 1997. Tracking changes in HIV-1 envelope quasispecies using DNA heteroduplex analysis. Methods **12:**348–354.
10. **Deng, H., R. Liu, W. Ellmeier, S. Choe, D. Unutmaz, M. Burkhart, P. Di Marzio, S. Marmon, R. E. Sutton, C. M. Hill, C. B. Davis, S. C. Peiper, T. J. Schall, D. R. Littman, and N. R. Landau.** 1996. Identification of a major co-receptor for primary isolates of HIV-1. Nature **381:**661–666.
11. **Fouchier, R. A., M. Groenink, N. A. Kootstra, M. Tersmette, H. G. Huisman, F. Miedema, and H. Schuitemaker.** 1992. Phenotype-associated sequence variation in the third variable domain of the human immunodeficiency virus type 1 gp120 molecule. J. Virol. **66:**3183–3187.
12. **Ganeshan, S., R. E. Dickover, B. T. Korber, Y. J. Bryson, and S. M. Wolinsky.** 1997. Human immunodeficiency virus type 1 genetic evolution in children with different rates of development of disease. J. Virol. **71:**663–677.
13. **Harouse, J. M., C. Buckner, A. Gettie, R. Fuller, R. Bohm, J. Blanchard, and C. Cheng-Mayer.** 2003. $CD8^+$ T cell-mediated CXC chemokine receptor 4-simian/human immunodeficiency virus suppression in dually infected rhesus macaques. Proc. Natl. Acad. Sci. USA **100:**10977–10982.
14. **Harouse, J. M., A. Gettie, T. Eshetu, R. C. Tan, R. Bohm, J. Blanchard, G. Baskin, and C. Cheng-Mayer.** 2001. Mucosal transmission and induction of simian AIDS by CCR5-specific simian/human immunodeficiency virus SHIV(SF162P3). J. Virol. **75:**1990–1995.
15. **Harouse, J. M., A. Gettie, R. C. Tan, J. Blanchard, and C. Cheng-Mayer.** 1999. Distinct pathogenic sequela in rhesus macaques infected with CCR5 or CXCR4 utilizing SHIVs. Science **284:**816–819.
16. **Harrowe, G., and C. Cheng-Mayer.** 1995. Amino acid substitutions in the V3 loop are responsible for adaptation to growth in transformed T-cell lines of a primary human immunodeficiency virus type 1. Virology **210:**490–494.
17. **Ho, S. H., L. Shek, A. Gettie, J. Blanchard, and C. Cheng-Mayer.** 2005. V3 loop-determined coreceptor preference dictates the dynamics of $CD4^+$-T-cell loss in simian-human immunodeficiency virus-infected macaques. J. Virol. **79:**12296–12303.
18. **Hwang, S. S., T. J. Boyle, H. K. Lyerly, and B. R. Cullen.** 1991. Identification of the envelope V3 loop as the primary determinant of cell tropism in HIV-1. Science **253:**71–74.
19. **Jeanmougin, F., J. D. Thompson, M. Gouy, D. G. Higgins, and T. J. Gibson.** 1998. Multiple sequence alignment with Clustal X. Trends Biochem. Sci. **23:**403–405.
20. **Kimura, M.** 1980. A simple method for estimating evolutionary rates of base substitutions through comparative studies of nucleotide sequences. J. Mol. Evol **16:**111–120.
21. **Kiselyeva, Y., R. Nedellec, A. Ramos, C. Pastore, L. B. Margolis, and D. E. Mosier.** 2007. Evolution of CXCR4-using human immunodeficiency virus type 1 SF162 is associated with two unique envelope mutations. J. Virol. **81:**3657–3661.
22. **Koot, M., I. P. Keet, A. H. Vos, R. E. de Goede, M. T. Roos, R. A. Coutinho,**

F. Miedema, P. T. Schellekens, and M. Tersmette. 1993. Prognostic value of HIV-1 syncytium-inducing phenotype for rate of $CD4^+$ cell depletion and progression to AIDS. Ann. Intern. Med. **118:**681–688.
23. **Kwong, P. D., R. Wyatt, J. Robinson, R. W. Sweet, J. Sodroski, and W. A. Hendrickson.** 1998. Structure of an HIV gp120 envelope glycoprotein in complex with the CD4 receptor and a neutralizing human antibody. Nature **393:**648–659.
24. **Lederman, M. M., A. Penn-Nicholson, M. Cho, and D. Mosier.** 2006. Biology of CCR5 and its role in HIV infection and treatment. JAMA **296:**815–826.
25. **Liu, S. L., T. Schacker, L. Musey, D. Shriner, M. J. McElrath, L. Corey, and J. I. Mullins.** 1997. Divergent patterns of progression to AIDS after infection from the same source: human immunodeficiency virus type 1 evolution and antiviral responses. J. Virol. **71:**4284–4295.
26. **Luciw, P. A., E. Pratt-Lowe, K. E. Shaw, J. A. Levy, and C. Cheng-Mayer.** 1995. Persistent infection of rhesus macaques with T-cell-line-tropic and macrophage-tropic clones of simian/human immunodeficiency viruses (SHIV). Proc. Natl. Acad. Sci. USA **92:**7490–7494.
27. **Malenbaum, S. E., D. Yang, L. Cavacini, M. Posner, J. Robinson, and C. Cheng-Mayer.** 2000. The N-terminal V3 loop glycan modulates the interaction of clade A and B human immunodeficiency virus type 1 envelopes with CD4 and chemokine receptors. J. Virol. **74:**11008–11016.
28. **Michael, N. L., A. E. Brown, R. F. Voigt, S. S. Frankel, J. R. Mascola, K. S. Brothers, M. Louder, D. L. Birx, and S. A. Cassol.** 1997. Rapid disease progression without seroconversion following primary human immunodeficiency virus type 1 infection—evidence for highly susceptible human hosts. J. Infect. Dis. **175:**1352–1359.
29. **Miedema, F., M. Tersmette, and R. A. van Lier.** 1990. AIDS pathogenesis: a dynamic interaction between HIV and the immune system. Immunol. Today **11:**293–297.
30. **Montagnier, L., C. Brenner, S. Chamaret, D. Guetard, A. Blanchard, J. de Saint Martin, J. D. Poveda, G. Pialoux, and M. L. Gougeon.** 1997. Human immunodeficiency virus infection and AIDS in a person with negative serology. J. Infect. Dis. **175:**955–959.
31. **Moore, J. P., S. G. Kitchen, P. Pugach, and J. A. Zack.** 2004. The CCR5 and CXCR4 coreceptors—central to understanding the transmission and pathogenesis of human immunodeficiency virus type 1 infection. AIDS Res. Hum Retrovir. **20:**111–126.
32. **Nelson, J., T. Riddle, N. Shire, M. Sherman, K. Franco, and H. Sheppard.** 2007. Sequential turnover of *env* variants and co-receptor switching during HIV-1 chronic infection, abstr 252. 14th Conf. Retrovir. Opportunistic Infect., Los Angeles, CA.
33. **Polzer, S., M. T. Dittmar, H. Schmitz, and M. Schreiber.** 2002. The N-linked glycan g15 within the V3 loop of the HIV-1 external glycoprotein gp120 affects coreceptor usage, cellular tropism, and neutralization. Virology **304:**70–80.
34. **Regoes, R. R., and S. Bonhoeffer.** 2005. The HIV coreceptor switch: a population dynamical perspective. Trends Microbiol. **13:**269–277.
35. **Rizzuto, C., and J. Sodroski.** 2000. Fine definition of a conserved CCR5-binding region on the human immunodeficiency virus type 1 glycoprotein 120. AIDS Res. Hum Retrovir. **16:**741–749.
36. **Rizzuto, C. D., R. Wyatt, N. Hernandez-Ramos, Y. Sun, P. D. Kwong, W. A. Hendrickson, and J. Sodroski.** 1998. A conserved HIV gp120 glycoprotein structure involved in chemokine receptor binding. Science **280:**1949–1953.
37. **Rowland-Jones, S. L.** 2003. Timeline: AIDS pathogenesis: what have two decades of HIV research taught us? Nat. Rev. Immunol. **3:**343–348.
38. **Shankarappa, R., J. B. Margolick, S. J. Gange, A. G. Rodrigo, D. Upchurch, H. Farzadegan, P. Gupta, C. R. Rinaldo, G. H. Learn, X. He, X. L. Huang, and J. I. Mullins.** 1999. Consistent viral evolutionary changes associated with the progression of human immunodeficiency virus type 1 infection. J. Virol. **73:**10489–10502.
39. **Shioda, T., J. A. Levy, and C. Cheng-Mayer.** 1991. Macrophage and T cell-line tropisms of HIV-1 are determined by specific regions of the envelope gp120 gene. Nature **349:**167–169.
40. **van Rij, R. P., M. D. Hazenberg, B. H. van Benthem, S. A. Otto, M. Prins, F. Miedema, and H. Schuitemaker.** 2003. Early viral load and CD4+ T cell count, but not percentage of $CCR5^+$ or $CXCR4^+$ $CD4^+$ T cells, are associated with R5-to-X4 HIV type 1 virus evolution. AIDS Res. Hum Retrovir. **19:**389–398.
41. **Wei, X., J. M. Decker, S. Wang, H. Hui, J. C. Kappes, X. Wu, J. F. Salazar-Gonzalez, M. G. Salazar, J. M. Kilby, M. S. Saag, N. L. Komarova, M. A. Nowak, B. H. Hahn, P. D. Kwong, and G. M. Shaw.** 2003. Antibody neutralization and escape by HIV-1. Nature **422:**307–312.